# Early Eocene environmental development in the northern Peri-Tethys (Aktulagay, Kazakhstan) based on benthic foraminiferal assemblages and stable isotopes (O, C)

Arne Deprez[a]*; Steven Tesseur[a1]; Peter Stassen[a]; Simon D'haenens[a,2]; Etienne Steurbaut[a,b]; Christopher King[c]; Philippe Claeys[d]; Robert P. Speijer[a]

E-mail addresses: arne.deprez@ees.kuleuven.be; steven_tesseur@msn.com peter.stassen@ees.kuleuven.be; simon.dhaenens@yale.edu; etienne.steurbaut@naturalsciences.be; chrking@globalnet.co.uk; phclaeys@vub.ac.be; robert.speijer@ees.kuleuven.be

Affiliations:

[a]Department of Earth and Environmental Sciences, KU Leuven, Celestijnenlaan 200E, B-3001 Heverlee, Belgium

[b]OD Earth and History of Life, Royal Belgian Institute of Natural Sciences, Vautierstraat 29, B-1000 Brussels, Belgium

[c]16A Park Rd., Bridport DT6 5DA, United Kingdom

[d]Earth System Science, Vrije Universiteit Brussel, Pleinlaan 2, B-1050 Brussels, Belgium

[1]Present address: Research Unit Palaeontology, Ghent University, Krijgslaan 281 S8, 9000 Ghent, Belgium

[2]Present address: Present address: Department of Geology & Geophysics, Yale University, 210 Whitney Avenue, New Haven, CT 06511, United States.

*Corresponding author: Tel. +32 16 372195, Fax. +32 16 322980

## Abstract

The Aktulagay section in Kazakhstan provides an expanded northern Tethyan record of the middle Ypresian (calcareous nannoplankton zones NP11-13, ~54-50 Ma), including the Early Eocene Climatic Optimum (EECO). The marl sequence features a series of sapropel beds, observed throughout the Peri-Tethys, indicative of the basin-wide occurrence of episodic hypoxic events. In order to unravel the paleoenvironmental evolution at Aktulagay during this period of global warming, we investigated the benthic foraminiferal record by means of a detailed multivariate analysis of the >63 µm fraction, as well as through stable isotopic (C, O) investigations on excellently preserved benthic foraminiferal specimens.

The Alashen Formation (NP11 to lower NP12; ~54 to 52.5 Ma), in the lower part of the

sequence, contains a diverse assemblage of deep outer neritic (~200-250 m) benthic foraminifera, with common *Pulsiphonina prima* and *Paralabamina lunata*. The sea-floor conditions are interpreted as initially (54 Ma) well-ventilated and oligo- to mesotrophic, gradually changing to more eutrophic and oxygen-limited, culminating in more permanent low-oxygen conditions and eutrophy in the sapropel-bearing Aktulagay B1 unit (middle NP12; ~52.5-52 Ma). The latter conclusion is corroborated by the dominance of *Anomalinoides acutus* and *Bulimina aksuatica* and the lower diversity. Also the upward migration of endobenthic species to the sediment-water interface, as suggested by rising $\delta^{13}C_{endobenthic}$ values, supports this interpretation. A transgression, which flooded lowlands, might have caused this development. In the Aktulagay B2 unit (top NP12-NP13; ~52-50 Ma), benthic foraminiferal assemblages dominated by *Epistominella minuta* suggest an oligotrophic environment, with transient pulses of phytodetritus and moderate ventilation.

The Aktulagay B2 unit coincides with the peak temperature interval of the EECO, as indicated by its position close to the base of NP13 and rising $\delta^{13}C_{epibenthic}$ values. Large river plumes, episodically reaching the area, in a monsoonal climatic context, might explain this basin development. Although it is not unlikely that some of the observed patterns are related to long-term climate change, it can currently not be excluded that changing paleogeography and variable connections to the Tethys, Atlantic and the Arctic Ocean were responsible for the long-term period with dysoxia and anoxia during deposition of the sapropel beds at the Peri-Tethyan seafloor.

The evolution of the basin as observed in Aktulagay shows similarities to the evolution of the North Sea Basin as observed in Denmark, suggesting that these basins were connected during the Early Eocene.

keywords: Early Eocene; Benthic foraminifera; Paleoecology; Kazakhstan; Oxygen deficiency; Trophic conditions

## 1.  Introduction

The Eocene was the warmest period in the Cenozoic, characterized by rising temperatures up to the Early Eocene Climatic Optimum (EECO; Zachos et al., 2008). Superimposed on this warming trend, multiple transient warming events, of which the PETM is the most extreme example, can be identified (e.g., Kennett and Stott, 1991; Zachos et al., 2010). Whereas the record of early Eocene global warming towards the EECO, mainly based on geochemical proxies, is becoming well established, the biotic response to this long-term trend is poorly known. This study aims at filling this gap through the study of a benthic foraminiferal record of a mid-latitude section in the Northern Peri-Tethys.

The early Eocene northern Peri-Tethys (Fig. 1) was characterized by its position between north-south and east-west trending seaways (Akhmetiev, 2011). From the early Paleocene to the middle Eocene, the northern Peri-Tethys was connected to the Arctic region by a north-south corridor, known as the Turgai Strait (Dercourt et al., 2000; Akhmetiev, 2011; Iakovleva, 2011). The northern and southern parts of the corridor differed in fauna, flora and sedimentation patterns (Dercourt et al., 2000). Recent studies indicate also the existence of a northern Peri-Tethys connection with the North Sea Basin and the Atlantic during the early Eocene (Iakovleva et al., 2004; Knox et al., 2010; Steurbaut, 2011; King et al., 2013). The circulation patterns within these seaways and the exact history of these connections influencing Peri-Tethyan paleoenvironments remain still poorly constrained. In the Peri-Tethys, the PETM is characterized by sapropel (black shale) deposition (e.g. Gavrilov et al., 2003). Interestingly, during the late Ypresian (calcareous nannoplankton zones NP12-13), up to eight organic rich shale and marl beds, generally denoted as sapropels, were deposited in

the northern Peri-Tethys area (Oberhänsli and Beniamovski, 2000; Stupin, 2008). These sapropel beds mark an unusual 500 thousand year period of basin-wide recurrent oxygen deficiency.

The dynamic warm climate, the recurrent deposition of sapropel beds and the paleogeographic setting with connections to the Tethys, Arctic and Atlantic Oceans, provides a unique setting for studying the early Eocene paleoenvironmental development of the northern Peri-Tethys. The stratigraphy of the Aktulagay section (Western Kazakhstan) was recently described in detail, combined with a general interpretation of depositional environments and depositional sequences, based on sedimentology, microfauna, macrofauna, nannofossils and dinocysts (King et al., 2013). This work forms the foundation for an in-depth quantitative and statistical evaluation of the benthic foraminiferal sequence. Together with stable isotopic data of excellently preserved benthic foraminifera this provides a great opportunity to characterize paleoenvironmental and biotic changes during early Eocene long-term global warming in a mid-latitude epicontinental basin.

## 2. Geologic setting and stratigraphy

### 2.1. The Aktulagay section

The Aktulagay section (47°32'31.47" N, 55°09'13.75" E; Fig. 1), located about 100 km NE of the town of Kulsary, is exposed in a steep slope on the western flank of the Aktulagay hills (Steurbaut, 2011). The section was logged and sampled for a stratigraphic study between 2000 and 2003 (King et al., 2013). Based on a study of this and other outcrops in the Pre-Caspian area, these authors proposed to subdivide the Eocene part into the Alashen Formation (0-13.45 m), composed of marl and calcareous clay, the Aktulagay Formation (13.45-23.57 m), containing marl, clay and sapropelitic clay, and the more silty overlying Tolagaysor Formation (23.57-56.20 m; King et al., 2013; Fig. 2). This study focuses on the Alashen and Aktulagay Formations for which a total of 24 samples were analyzed (Fig. 3, lowermost sample 0-0.10 m was not studied because of strong reworking). The sampling was carried out initially for stratigraphic purposes, and some of the material was already exhausted during the previous study by King et al. (2013), consequently, a higher resolution study of parts of the sequence was not possible.

### 2.2. Biostratigraphy

A detailed overview of the biostratigraphy of the Aktulagay section can be found in King et al. (2013). The most important findings are reported here. Since most of the nannofossil units identified in the North Sea Basin can be recognized in the Aktulagay section, the nannofossil subzonation of the North Sea Basin is applied here (Steurbaut, 1998), as a subzonation of the zonal scheme of Martini (1971) (Fig. 3). Ages in this paper are based on the Geologic Time Scale of the Paleogene (Vandenberghe et al., 2012), with corrections on the ages of the nannoplankton zones by Pirkenseer et al. (2013). Ages are inferred from bio- and chemostratigraphic correlation (Fig. 4). The lowest part of the section, unit A1 (0-0.20 m) belongs to nannoplankton subzone NP10b. It is separated by a hiatus from the overlying unit A2 (0.20-10.80 m; ~54-52.75 Ma; NP11 − lowest NP12), which is thought to include 13 omission surfaces. Unit A2 is separated from unit A3 (10.80-13.45 m; ~52.75-52.5 Ma; lower NP12) by another omission surface. A further omission surface is detected at 12.80 m. The boundary between zones NP11 and NP12 is found at 9.0 m (in unit A2), identified by the first (rare) occurrence of *Discoaster lodoensis*.

At the base of unit B1 (13.45-16.22 m; ~52.5-52 Ma; mid NP12) a hiatus may be present,
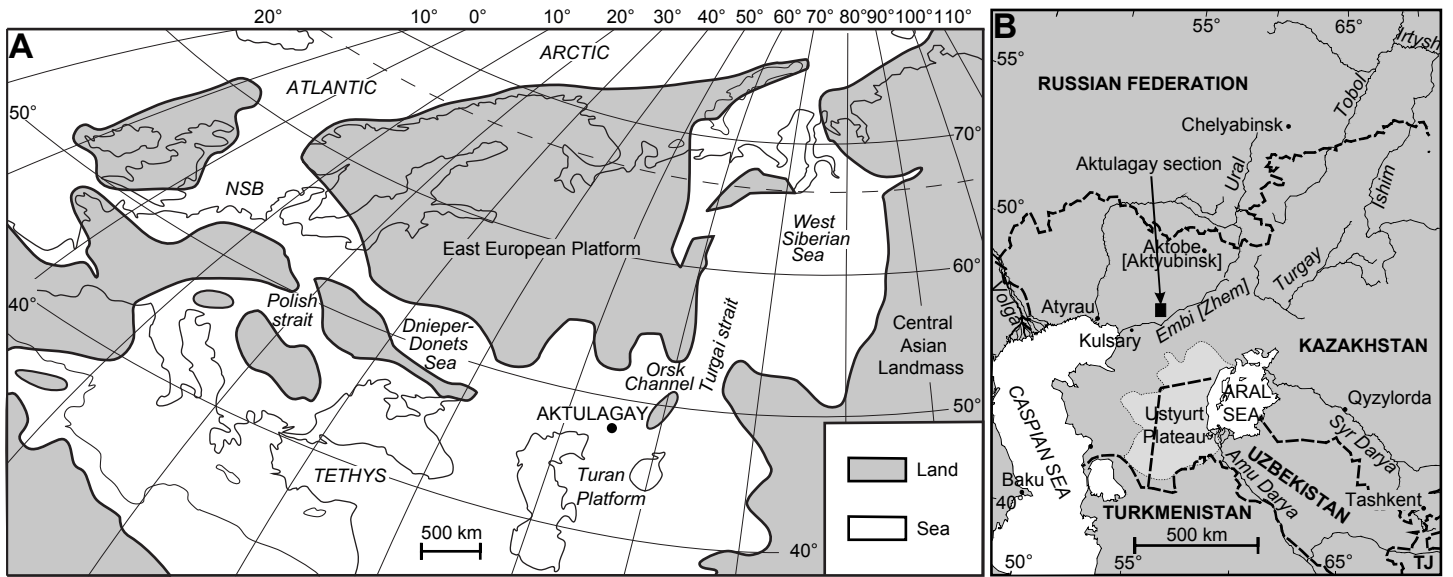
Fig. 1. Location of the Aktulagay section. (A) Early Eocene paleogeography after Steurbaut (2011). The Peri-Tethys is in this reconstruction connected to the Tethyan, Arctic and Atlantic ocean. NSB = North Sea Basin (B) Present-day location (modified from King et al., 2013).
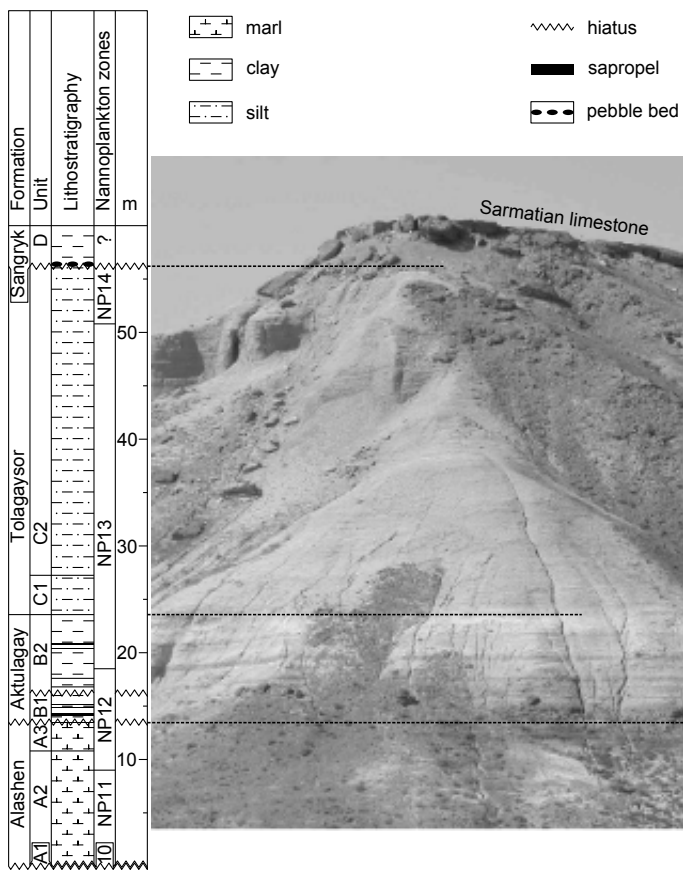


Fig. 2. Photograph and lithostratigraphic column of the Aktulagay section (King et al., 2013; Steurbaut, 2011). Nannofossil zonal scheme by Martini (1971).
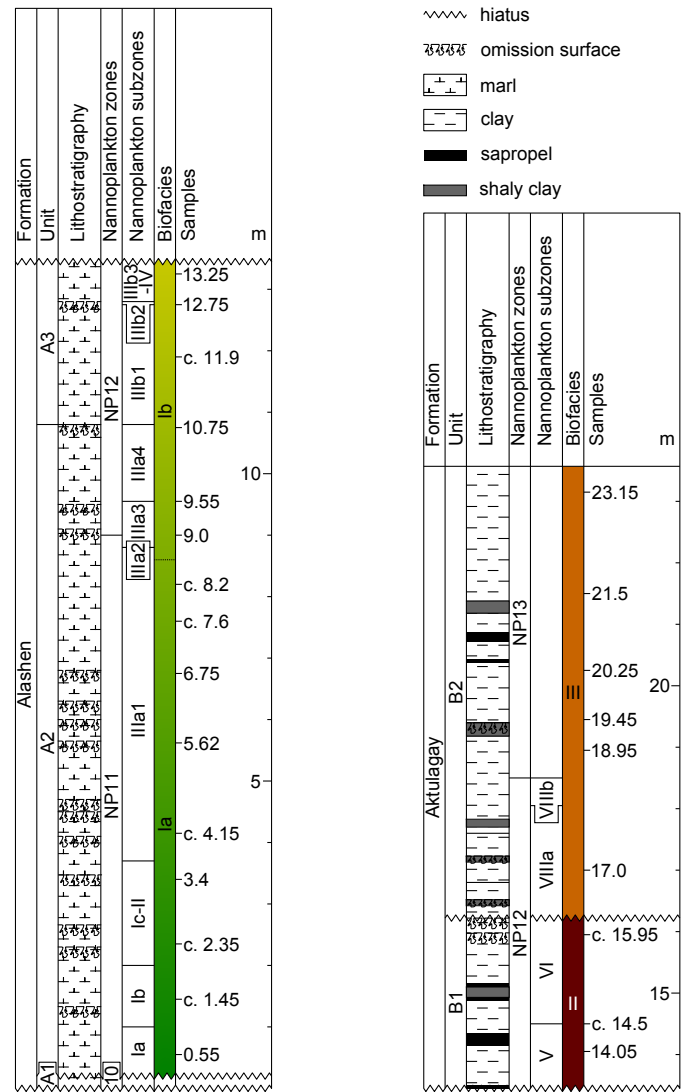


Fig. 3. Position of samples on detailed lithological logs and biostratigraphical logs by King et al. (2013). Nannofossil zonation scheme by Martini (1971) NSB NP subzones: North Sea Basin Nannoplankton subzones (Steurbaut, 1998).

indicated by the absence of calcareous nannoplankton subzone IV of the North Sea Basin succession. The base of unit B2 (16.22-23.57 m; ~52-50 Ma; top NP12-NP13) is characterized by a hiatus with a duration of at least ca. 55 kyr, based on the absence of nannofossil subzone VII (King et al., 2013). The top of Zone NP12 (defined by the last occurrence of *Tribrachiatus orthostylus*) is identified at 18.50 m.

## 3. Methods

### 3.1. Micropaleontologic analyses

Samples were weighed, soaked in distilled water and dried at 50°C. After drying, they were soaked again in a 50 g/l sodium carbonate solution for 6 to 24 hours. After this preparation, samples were gently washed with tap water over a 63 μm sieve, dried and the fraction >63 μm was weighed. Clean residues were obtained after one washing cycle only. Data in this study are based on analysis of a representative aliquot of the fraction >63 μm, while the foraminiferal data in the mainly stratigraphic study by King et al. (2013) are based on the >120 μm fraction.

Semi-quantitative estimates of the number of various components in the samples were made, such as ostracods and large dinoflagellate cysts (>63 μm). Also a qualitative estimate of the preservation was made. To calculate the benthic and planktic foraminiferal numbers per gram of sediment (BFN and PFN, respectively) and the percentage of planktic foraminifera relative to the total number of foraminifera (%P, commonly denoted as P/B ratio), the foraminifera were counted from a representative split, using an ASC micro-splitter. Quantitative assemblage data are obtained from a split of the >63 μm fraction and mounted on reference slides (>250-300 counts).

Taxonomic assignments were based on Brotzen (1948), Berggren and Aubert (1975), Aubert and Berggren (1976), Van Morkhoven et al. (1986), Loeblich and Tappan (1988), Willems (1988), Jenkins and Murray (1989), Speijer (1994), Bugrova (2005), Clemmensen and Thomsen (2005), Stassen (2012) and Stassen et al. (2012a).

Many taxa have been described in Russian-language literature with holotypes from the Peri-Tethys. Direct comparison of these taxa to those described in Europe and Africa was difficult, but it is clear that there is significant synonymy. We made a considerable effort to evaluate synonymies and priorities using the Ellis and Messina catalogue ([www.micropress.org/em](http://www.micropress.org/em)). Synonymous names are incorporated in the second column of the alphabetic list of taxa in the Supplementary information (Appendix B).

For each sample, Buzas and Gibson's evenness ($e^H/S$), Shannon diversity (H) and species richness (S) were calculated based on the complete dataset with absolute counts (see Hammer, 2014 for formulas). Hierarchical cluster analysis (CA) was carried out in R-mode (groupings of taxa). The unweighted pair-group average algorithm and the distance measure Pearson correlation were used. The average linkage algorithm is recommended for ecological data, it produces groups in which all members of the group are close to each other (Hammer and Harper, 2006). The Pearson correlation distance measure groups species with similar patterns of high and low relative abundances, independent of how abundant a species is in general. Finally Detrended Correspondence Analysis (DCA) was run to identify the environmental factors governing the benthic foraminiferal distribution. DCA is the technique used to ordinate samples and taxa, in which taxa have a unimodal response to the environmental gradient. Each taxon is most abundant at a different value for an environmental parameter (e.g. dysoxic conditions), becoming rarer for both lower and higher values (e.g. more anoxic and more oxic). Ordination in a DCA helps to find the main environmental gradients governing the

benthic foraminiferal distribution. All statistic analysis was based on PAST software (Hammer et al., 2001). For both the CA and the DCA a dataset containing only the taxa with a relative abundance higher than 2.5 % in at least one sample were used.

## 3.2. Stable isotope analysis

Stable isotopes were measured on monospecific samples of excellently preserved (glassy) *Cibicidoides decoratus*, *Anomalinoides acutus*, *A. zitteli*, *Uvigerina elongata* and *Bulimina aksuatica* in the 63-125, 125-180, 180-250 or 250-300 µm size fraction or a combination of 2 of these (Appendix B). Specimens were cleaned in an ultrasonic bath, except for some *U. elongata* and *B. aksuatica* samples, which were judged too fragile to survive this treatment. A test with uncleaned and cleaned *Aragonia aragonensis* revealed that even without cleaning, the result did not significantly differ between specimens treated with or without ultrasound. The samples were analyzed using a ThermoFinnigan Delta$^{plus}$ XL mass spectrometer equipped with an automated Kiel III carbonate preparation line at the Vrije Universiteit Brussel (VUB). Analytical uncertainties (1σ) were ≤0.07 ‰ for $\delta^{13}C$ and ≤0.11 ‰ for $\delta^{18}O$, except for one measurement (*B. aksuatica* at 20.25 m) with analytical uncertainty 0.14 ‰ for $\delta^{18}O$, due to insufficient material. This sample was used in the analysis, because the $\delta^{18}O$ value is similar to the nearby sample at 19.45 m and the uncertainty is still smaller than variation between samples.

The epibenthic record is mainly based on *C. decoratus*. In samples lacking this species, *A. acutus* or *A. zitteli* was used and the result was corrected for constant species-specific offsets with the isotopic signature of *C. decoratus*. Microhabitat associations of these epibenthic species were based on morphotype classifications (Corliss and Chen, 1988) and a consistent $\delta^{13}C$ offset between assumed epibenthic and endobenthic species (Fig. 5 and unpublished results of other species). Due to microhabitat effects, epibenthic species generally have a higher $\delta^{13}C$ value than endobenthic species (McCorkle et al., 1997; Fontanier et al., 2006). Both *Cibicidoides* and *A. acutus* have previously been used to generate epibenthic isotope records (e.g. Cramer et al., 1999; Zachos et al., 2001; Stassen et al., 2012b). Correction factors were calculated by linear regression in samples in which both species co-occur. Values of *A. acutus* are corrected with a factor +0.32 ‰ for $\delta^{18}O$ and +0 ‰ for $\delta^{13}C$, values of *A. zitteli* with a factor -0.04 ‰ for $\delta^{18}O$ and -0.14 ‰ for $\delta^{13}C$. *Bulimina aksuatica* is assumed to record a deep and *U. elongata* a shallow endobenthic signature. Both species have an endobenthic morphotype. *Bulimina aksuatica* has generally a $\delta^{13}C$ offset of >1 ‰ with epibenthic species (Fig. 5) and has a low $\delta^{13}C$ value compared to other species with an endobenthic morphotype in Aktulagay (unpublished results). *Uvigerina elongata* generally has a ~1 ‰ $\delta^{13}C$ offset with epibenthic species, but values are consistently higher than values for *B. aksuatica* (Fig. 5). Carbon isotopic values of *Uvigerina elongata* are on the high end, but still similar to other species with an endobenthic morphotype in Aktulagay (unpublished results). Temperature calculations for epibenthos were performed with a correction of 0.45 ‰ for equilibrium calcite (Zachos et al., 2001; Katz et al., 2003), a $\delta^{18}O_{sw-mean}$ (V-SMOW) value of -0.9 ‰ (Zachos et al., 1994; Cramer et al., 1999; Pearson et al., 2007; Tindall et al., 2010; Roberts et al., 2011) and the paleotemperature equation of Lynch-Stieglitz et al. (1999) for *Cibicidoides* and *Planulina*.

# 4. Results

## 4.1. Foraminiferal preservation

Planktic foraminifera are generally less resistant to dissolution than benthic foraminifera (e.g. Nguyen et al., 2009). The percentage planktic foraminifera relative to the total number of

foraminifera (%P) is generally high, with minima not correlated to minima in number of foraminifera (Fig. 5), except for the first sample (0-0.10 m), which was not studied quantitatively. The high number of planktonic foraminifera indicates that most samples were not significantly affected by dissolution.

The influence of dissolution can also be assessed by comparing patterns of resistant and susceptible benthic foraminifera. *Globocassidulina subglobosa*, *Cibicidoides rigidus*, *Nuttallides truempyi*, *Valvulineria scrobiculata*, *Anomalinoides zitteli*, *Osangularia plummerae* and *Lenticulina* spp. are more resistant to dissolution, while *Uvigerina elongata*, *Valvalabamina planulata*, *Stilostomella* spp., miliolids, Nodosariacea and Buliminacea appear to be more prone to dissolution (Corliss and Honjo, 1981; Widmark and Malmgren, 1988; Nguyen et al., 2009). Dissolution resistant and dissolution susceptible species don't follow opposite relative abundance patterns in Aktulagay (Fig. 6). Every faunal cluster (Fig. 7), except the small cluster B, contains both species resistant and species susceptible to dissolution. Dissolution resistant and susceptible species are often positively correlated, within the same cluster (e.g. *Anomalinoides zitteli* with *Bulimina mitgarziana*, *Quinqueloculina* spp. and *Uvigerina elongata*, r=0.51, p=0.004)

Most benthic foraminifera in the Aktulagay section are excellently preserved, but some show subtle signs of dissolution. Yet, all specimens reveal original test features such as sutures and pores and are translucent. Detailed SEM study (Plates 1 and 2) reveals minor breakage or etching as well as some rare overgrowth from precipitation of secondary calcite on a few less well-preserved specimens. These were not selected for isotope analysis. SEM images of specimens of the same quality as those used for stable isotope analysis show smooth tests, open pores and no indications of secondary calcite. Benthic foraminiferal preservation seems just as excellent as the best preserved specimens figured in the foraminiferal preservation study by Sexton and Wilson (2009).

## 4.2. Faunal and paleoenvironmental indices

Planktic (200-70 000 PFN/g) and benthic (400-10 000 BFN/g) foraminiferal numbers (Fig. 5) are generally higher in the lower part of the section (30 000 PFN/g, 5 000 BFN/g), except for the basal sample at 0-0.10 m (200 PFN/g, 400 BFN/g), which shows reworking and dissolution. %P varies from 50 to 90 %, with the highest values found at the base, followed by an upward decreasing trend. Ostracods are common to abundant in the entire section, except from 6.75 to 8.20 m and 14.05 to 15.95 m, where they are absent (Fig. 5). Large dinocysts (>63 μm) are particularly abundant in the washed residues from 19.45 to 20.25 m.

In total, 88 benthic foraminiferal species and 54 genera were distinguished in the studied interval. The most abundant species (Fig. 6) are typical for Paleocene to early Eocene Midway-type shelf assemblages (Berggren and Aubert, 1975) and have also been observed in southern Tethyan marginal basins (e.g. Speijer, 1994). However, some typical deep-sea species (e.g., *Nuttallides truempyi* and *Aragonia aragonensis*) are observed in small numbers in some intervals, suggesting deep-shelf (~200-250 m paleodepth) deposition. These deep-sea species can also occur at relatively shallow depth in oligotrophic parts of epicontinental basins (Speijer and Schmitz, 1998). P/B ratios are in the same range as for studies in similar water depth in the southern Tethys (Speijer and Schmitz, 1998; Ernst et al., 2006; Stassen et al., 2012c). Shannon diversity is generally fairly high, with an average value of 3. Three episodes show lower diversity, from 4.15 to 8.20 m, from 14.05 to 15.95 m, and from 19.45-20.25 m (Fig. 5).

The most abundant species in the high diversity samples are *Pulsiphonina prima*, *Paralabamina lunata* and *Anomalinoides* cf. *praeacutus*. However, these species reach higher
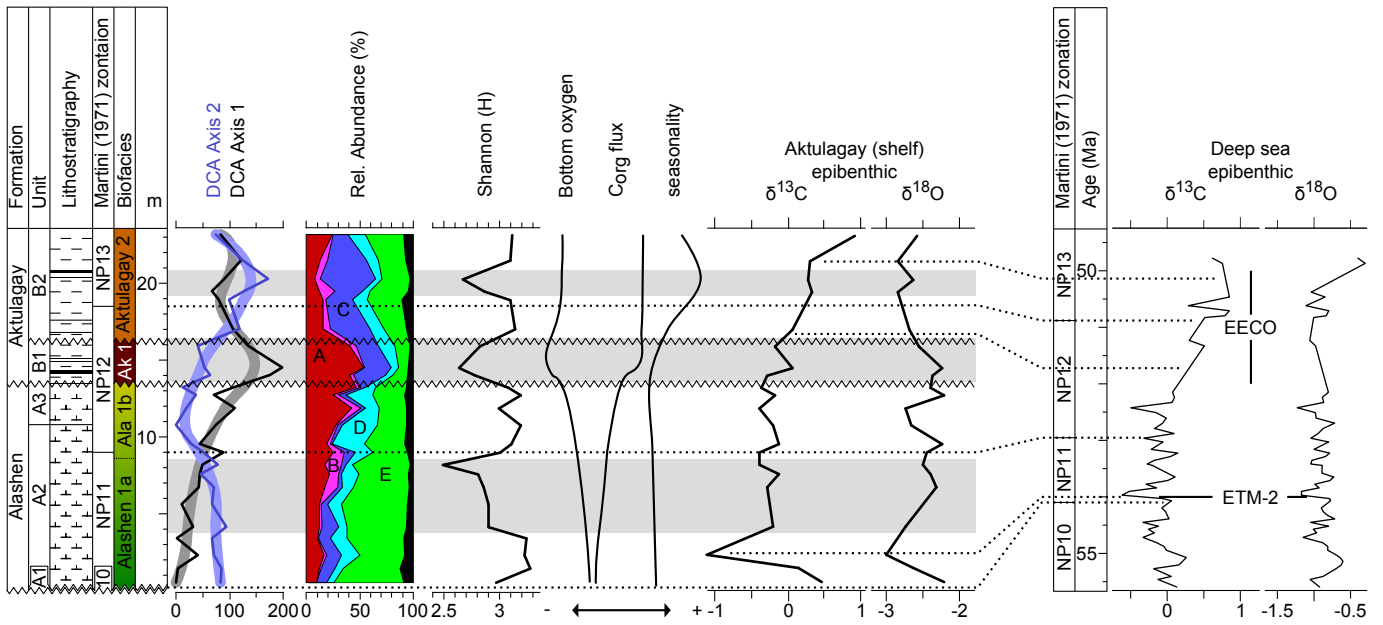
Fig. 4. Summary of paleoenvironmental indicators and interpretations based on benthic foraminifera and correlation with the deep-sea record of DSDP Site 550 (Charisi and Schmitz, 1996), using the nannofossil zonal scheme by Martini (1971) and comparison of the isotopic patterns. The position of ETM2 in DSDP Site 550 is based on D'haenens et al. (2014). The plotted time scale is according to GTS2012 (Vandenberghe et al., 2012), with correction of nannoplankton zones according to Pirkenseer et al. (2013).
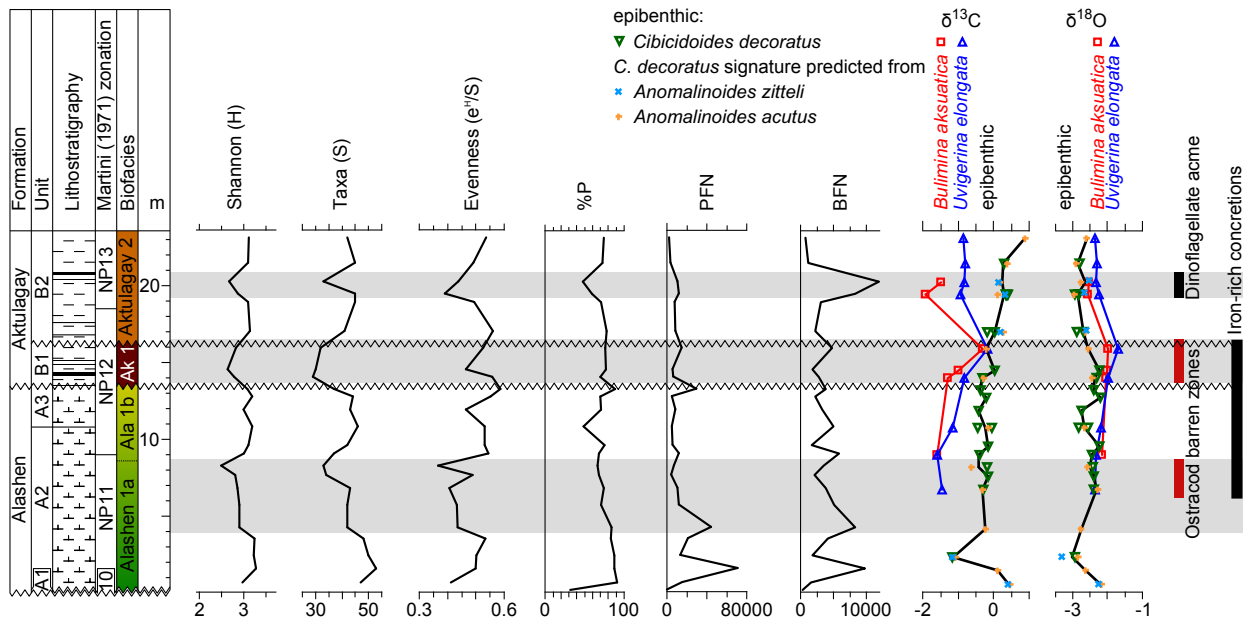


Fig. 5. Foraminiferal assemblage parameters: Taxa (S), Shannon diversity (H), Buzas and Gibson's Evenness (eH/S), percentage of planktic foraminifera (%P), benthic (BFN) and planktic (PFN) foraminiferal numbers per gram. Isotope signatures for Bulimina aksuatica (deep endobenthic), Uvigerina elongata (shallow endobenthic) and epibenthic species.
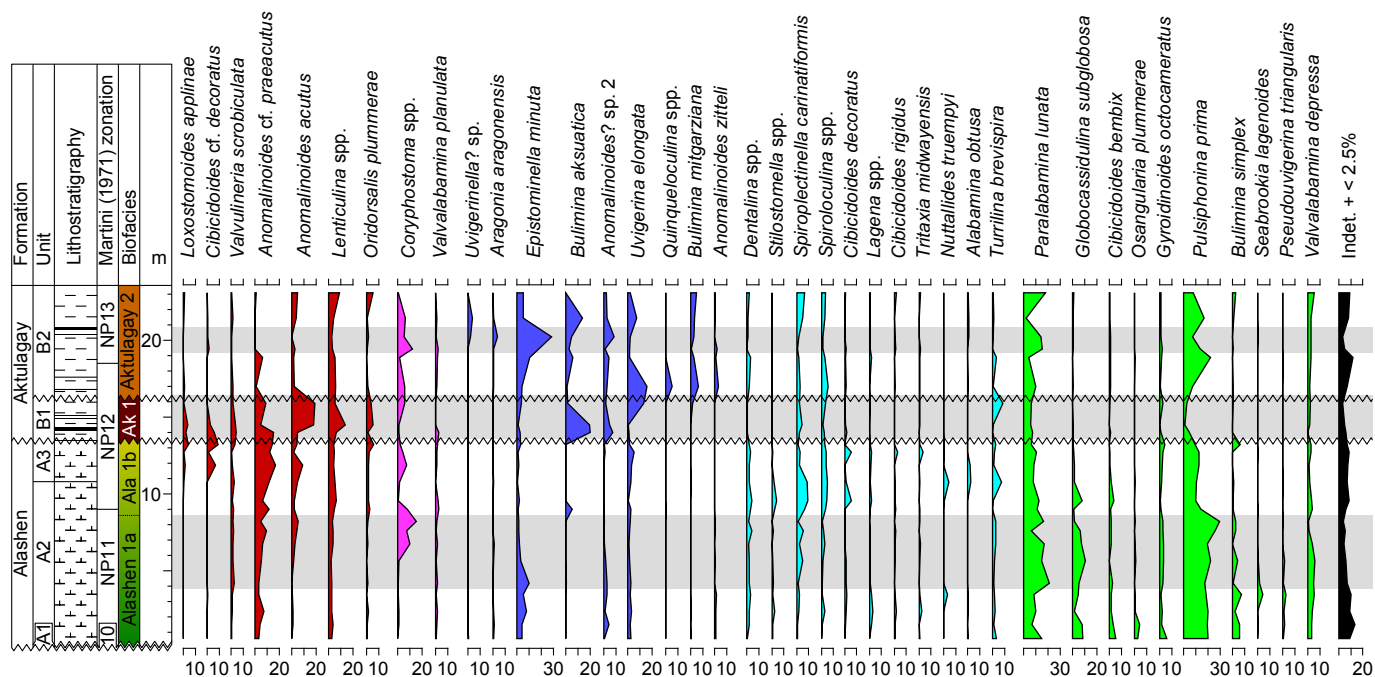
Fig. 6. Relative abundance patterns of benthic foraminifera through the Aktulagay section. Arrangement of taxa and coloration is the same as for cluster analysis (Fig. 7).
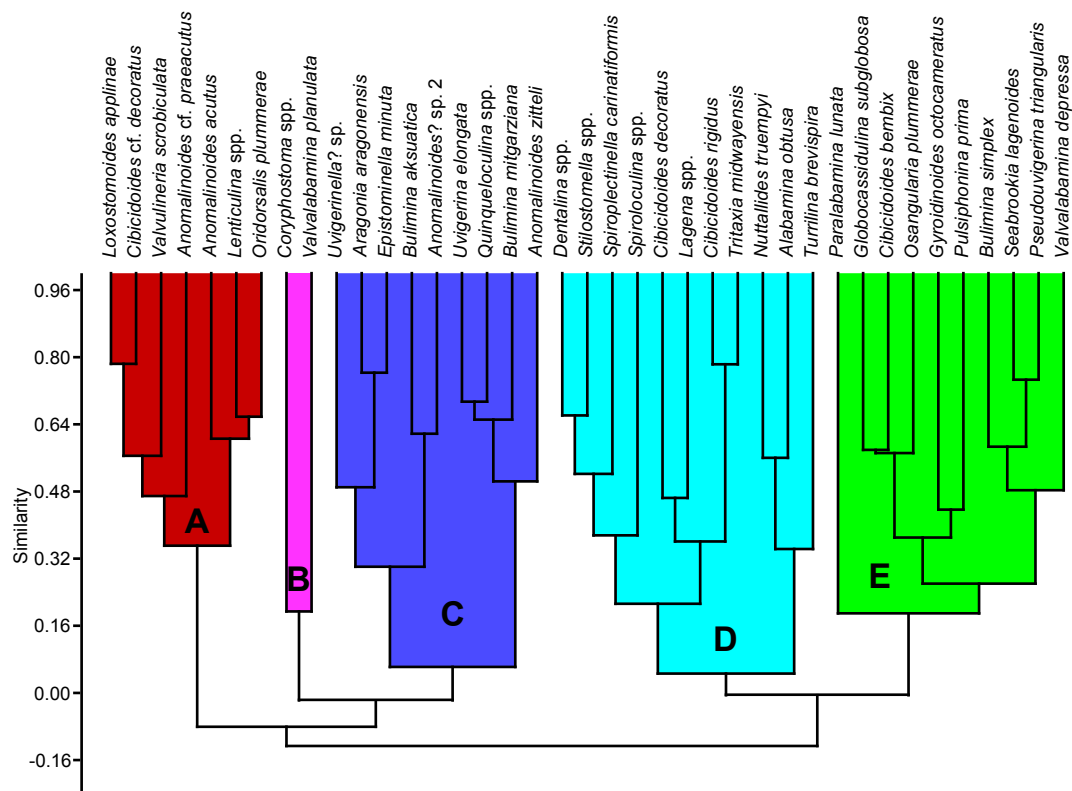


Fig. 7. Result of R-mode clustering. 5 different faunal clusters are differentiated based on the abundance patterns in the Aktulagay section. Cluster A contains species occurring opportunistically in low-oxygen environments, cluster B species in outer neritic to bathyal environments, C species associated with high transient food supply, without link with low oxygen concentrations, D contains species with epi- and endobenthic morphotypes typical for outer neritic conditions and E contains species most abundant in oligo-mesotrophic circumstances with sufficiently high oxygen concentrations.

relative abundances outside of the high diversity interval. High diversity samples also contain many species in low abundance (<2.5 %) (Fig. 6). The first diversity drop (4.15-8.20 m) is characterized by a drop in all diversity indices and an increase in relative abundance of *Coryphostoma* spp., *P. prima* and *P. lunata* as well as a decrease in low-abundance species (<2.5 %). Planktic and benthic foraminiferal numbers, as well as %P, follow the same decreasing trend through the Alashen Formation, without deviations from this trend during the first diversity drop.

The second low-diversity interval from 14.05 to 15.95 m is especially notable in species richness (S; section 3.1) and in the Shannon diversity, but Buzas and Gibson's Evenness ($e^H/S$), PFN, BFN and %P are rather stable (Fig. 5). Dominant species in these samples are *Bulimina aksuatica* and *Anomalinoides acutus*. *Paralabamina lunata* and *P. prima* decrease in abundance (Fig. 6).

Samples at 19.45 m and 20.25 m are characterized by a higher relative abundance of *Epistominella minuta*. *Pulsiphonina prima* and *A.* cf. *praeacutus* have a lower relative abundance in these samples (Fig. 6). The diversity drop at this level is associated with a sharp rise in benthic foraminiferal numbers, together with stable planktic foraminiferal numbers, leading to a decrease of %P (Fig. 5).

## 4.3. Faunal Clusters

The taxa are subdivided into 5 clusters, assigned A to E (Fig. 7; cumulative percentage for all clusters are shown in Fig. 4). The ecological interpretation can be found in the supplementary information (Appendix A). For each cluster, the quantitatively most important taxa are given between brackets. The taxa of faunal cluster A (mainly *A.* cf. *praeacutus* – *Lenticulina* spp. – *A. acutus*) show a gradual increase in relative abundance to reach a maximum at 14.05 to 15.95 m (52 % at 14.50 m). After reaching maximum values, their relative abundance decreases dramatically, until a minimum at 20.25 m (5 %).

The benthic foraminifera of faunal cluster B (mainly *Coryphostoma* spp.) only reach 10 % of relative abundance at 6.75 to 9.00 m and at 19.45 m. The maximum relative abundance of species in faunal cluster C (mainly *E. minuta* – *Uvigerina elongata* – *B. aksuatica*) is reached in the upper part of the section, with a peak of 52 % at 20.25 m.

The maximum in relative abundance of faunal cluster D (mainly *Spiroplectinella carinatiformis* – *Spiroloculina* spp.) is reached between 9.00 and 12.75 m. At 10.75 m this cluster shows a peak value of 34 %. Faunal cluster E (mainly *P. prima* – *P. lunata* – *Globocassidulina subglobosa* – *Valvalabamina depressa*) has the highest relative abundance, which is maximal at the base of the section with a relative abundance of 66 % at 0.55 m. The relative abundance gradually decreases to a minimum of 9 % at 14.50 m, after which it rises again to values around 30 %. This cluster includes the two most common taxa in this dataset: *P. prima* (average 14 %) and *P. lunata* (11 %).

## 4.4. Biofacies

Samples are assigned to biofacies based on detrended correspondence analysis (DCA; Fig. 8). Axis 1 has a detrended eigenvalue of 0.24, and axis 2 of 0.13. Samples at 14.05, c.14.50 and c.15.95 m (Aktulagay 1 Biofacies) are separated from all other samples. Samples below (Alashen 1 Biofacies) and above (Aktulagay 2 Biofacies) this level have different loadings on the two DCA axes and are grouped in 2 separate biofacies. The Aktulagay 2 Biofacies is more similar to the Alashen 1 Biofacies than to the Aktulagay 1 Biofacies. These biofacies correspond to lithostratigraphic units identified by King et al. (2013).
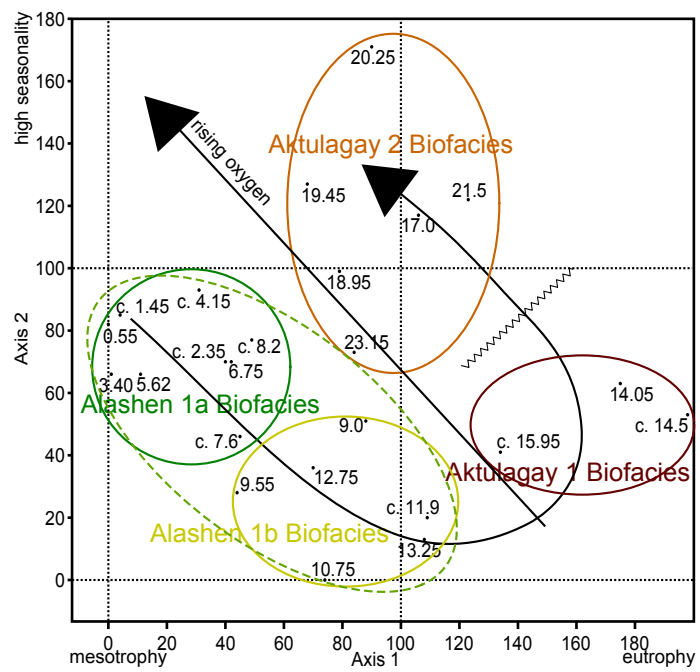
Fig. 8. Result of the DCA for samples. The division in biofacies and the trendline are indicated. Delineated biofacies correspond to the Alashen Formation, Aktulagay Formation, unit B1 and Aktulagay Formation, unit B2.

Alashen 1 Biofacies (0.20-13.45 m, NP11 and base of NP12): Faunal cluster E is quantitatively most important (on average, species combined in faunal cluster E account for 45 % in this biofacies; Fig. 4). Faunal clusters A (19 %) and D (16 %) also contribute substantially. A general trend from samples with low scores on axis 1 and intermediate scores on axis 2 to samples with intermediate scores on axis 1 and low scores on axis 2 can be observed, allowing a subdivision into Alashen 1a and 1b Biofacies (Fig. 8). This coincides with an increase in relative abundance of taxa of faunal clusters A (from 12 % in Alashen 1a Biofacies to 29 % in Alashen 1b Biofacies) and D (from 12 % in Alashen 1a Biofacies to 22 % in Alashen 1b Biofacies) and a decrease in relative abundance of faunal cluster E (from 55 % in Alashen 1a Biofacies to 31 % in Alashen 1b Biofacies).

Aktulagay 1 Biofacies (13.45-16.22 m, middle NP12): Taxa in faunal cluster A are most abundant (on average they account for 43 %). Species of Clusters B (3 %), D (10 %) and E (13 %) show a minimum relative abundance in this biofacies. Species of Cluster C (26 %) show a major increase, with peak values of *B. aksuatica, Anomalinoides*? sp. 2 and *U. elongata* (Fig. 6). On the DCA plot, the samples of this biofacies have highest scores on the first axis and rather low scores on the second axis. This biofacies coincides with an interval without ostracods.

Aktulagay 2 Biofacies (16.22-23.57 m, top NP12 to NP13): In this biofacies the species of cluster C (on average 33 %) and E (30 %) are most abundant (Fig. 4). Cluster A taxa have their lowest relative abundance in this interval (12 %) and cluster D taxa have an intermediate value (11 %). The Aktulagay 2 Biofacies samples reach high scores on the second DCA axis and intermediate scores on the first axis. In the samples with the highest scores on the second DCA axis (20.25 m and to a lesser extent 19.45 m) abundant large (>63 μm) dinocysts were observed in the washed residue.

## 4.5. Stable isotopes

Epibenthic $\delta^{13}$C values (Fig. 5) generally vary between -0.6 and 0.5 ‰, except for the sample at 2.35 m and the uppermost sample. The middle part of the section (4-14 m; NP11-12) shows stable values (-0.3 ‰). In the overlying sequence, $\delta^{13}$C values gradually increase upwards, reaching a maximum value at 23.15 m (0.9 ‰; NP13). Although the resolution is limited, the lowermost part of the section appears to reveal a negative carbon isotope excursion with $\delta^{13}$C values decreasing from 0.5 ‰ at 0.55 m (base NP11) to -1.1 ‰ at 2.35 m (lower NP11). These minimal values are observed in all three measured species (*C. decoratus, A. acutus and A. zitteli;* Fig. 5), giving similar values after correction for species-specific effects. SEM images show that preservation of the foraminifera in this sample is as good as in the other samples (Section 4.1 and Plate 1, Fig. 18d,e for *A. zitteli* from this sample).

Benthic $\delta^{18}$O values range from -2.2 to -3 ‰ (Fig. 5), pointing to temperatures of 18-22±1.8 °C at the outer shelf seafloor. Within this temperature range, three relatively warm (~20-22 °C) intervals can be distinguished at 1-5 m (lower NP11), 10-12 m (lower NP12) and 15-23 m (upper NP12-NP13). The lowest $\delta^{18}$O value (-3.0 ‰) at 2.35 m coincides with the lowest $\delta^{13}$C value, and is also represented in all three species analyzed.

The $\delta^{18}$O signature of endobenthic species *B. aksuatica* and *U. elongata* is nearly constant throughout the section (Fig. 5). Values for both species are between -1.7 and -2.6 ‰. However, the $\delta^{13}$C signatures show more variation. The most prominent feature is the collapse of the offset between endobenthic and epibenthic species starting from about 11 m (start of lithologic unit A3), with almost equal $\delta^{13}$C values at 15.95 m (end of lithologic unit B1). The second feature is the offset between the $\delta^{13}$C value of *B. aksuatica* (deep endobenthic) and *U. elongata* (shallow endobenthic) in unit B2, while in the sample at 9.00 m there is no such

offset.

## 5.    Discussion

### 5.1.   Isotope stratigraphy

The epibenthic isotope records (Fig. 4) reveal considerable variation within the section. At 2.35 m a strong depletion of the carbon isotopic signature is noted, in a single sample. This carbon isotope excursion of >1.0 ‰ is confirmed by measurements on *C. decoratus*, *A. acutus* and *A. zitteli*. It is most likely related to one of the early Eocene Carbon Isotope Excursions (CIEs) (Cramer et al., 2003; Galeotti et al., 2010) and its association with a negative oxygen isotope excursion suggests that it may involve a hyperthermal event. Considering the magnitude of the CIE (1-1.5 ‰) and its position close to the basis of NP11, ETM2 (Lourens et al., 2005) is a likely candidate for this potential hyperthermal. Alternatively, this isotope excursion could represent a local phenomenon. A higher resolution record and tighter stratigraphic constraints (e.g. through magnetostratigraphy) would be needed to further evaluate this event. This potential hyperthermal is not associated with faunal or sedimentologic anomalies (Section 5.2), as oberved in the Dababiya section in Egypt (Stassen et al., 2012c). However, because of the low resolution of this study, transient environmental change due to this potential hyperthermal might be missed in this dataset.

The EECO starts at about 52 Ma, in middle NP12 and before the first occurrence (FO) of the dinoflagellate cyst *Ochetodinium romanum* (Vandenberghe et al., 2012). This FO is situated at the boundary between Aktulagay Formation units B1 and B2, associated with a hiatus (King et al., 2013). The start of the EECO is situated in unit B1, but the highest temperatures of the EECO are only reached at ~50-51 Ma (Zachos et al., 2001; Sexton et al., 2006). This time period can be correlated to unit B2. With the limits of our low resolution, isotopic correlation to the isotopic deep-sea record of Charisi and Schmitz (1996) appears to confirm this interpretation (Fig. 4). Apart from the potential hyperthermal, $\delta^{18}O$ values generally decrease by about 0.4 ‰ to the top of the Aktulagay section and $\delta^{13}C$ values are stable up to middle NP12, followed by a gradual 1 ‰ rise. The deep-sea record also shows generally decreasing $\delta^{18}O$ values during NP10, NP11 and NP12 to a minimum at the base of NP13. The deep-sea $\delta^{13}C$ record shows stable values from the base of NP11 to middle NP12 and then rising values to the base of NP13.

### 5.2.   Ecologic Analysis
### Alashen 1a Biofacies (NP11)

Ecologic analysis of biofacies is based on ecologic interpretations of faunal clusters, based on earlier studies (Appendix A). The high abundance of cluster E taxa suggests oligo-mesotrophy and well-ventilated bottom water conditions during deposition of the Alashen Formation. Most of the species are characteristic of outer neritic environments (100-200 m), with a large number of species in the 'deep outer neritic group 3' (~150-200 m) of Speijer and Schmitz (1998). The rare occurrence of the bathyal taxon *N. truempyi* suggests deposition in water depths of ~200-250 m. This water depth is consistent with the outer neritic - upper bathyal water depth interpreted by King et al. (2013).

The slight decrease of cluster E and C species together with the slight increase of cluster A species in the upper part of the Alashen 1a Biofacies suggests gradually decreasing oxygen concentrations. From the fact that cluster E (oligo-mesotrophy) and C (eutrophy) species both decrease in abundance, we infer that a higher food input is not the primary cause for this trend, although food levels most likely increased as well.

Samples from 4.15 to 8.20 m show a lower diversity (Fig. 5), but from the DCA (Fig. 8) it is clear that these samples do not deviate from the trend to lower oxygen concentrations and higher food levels. Various species reach their optimum (Fig. 6) at different levels. At first, species in the "<2.5 %" group and some less abundant species of cluster E reach their optimum. Above this, *E. minuta* and *B. simplex* reach their highest relative abundance. They are followed by the consecutive peaks of *P. lunata*, *G. subglobosa*, *P. prima* and *Coryphostoma* spp.

These consecutive abundance peaks could be explained by the TROX model (Jorissen et al., 1995; van der Zwaan et al., 1999). Higher food levels generate higher abundances of species at their optimum, whereas they significantly decrease when oxygen concentrations become limiting. The peak pattern could reflect the different oxygen tolerances of different species. The first species, especially *E. minuta* and *P. lunata* are most adapted to oxygenated sediments, while *P. prima* and *Coryphostoma* spp. can tolerate lower oxygen concentrations. Above these species optima the higher abundance of cluster A taxa follows (Alashen 1b Biofacies), with species possibly tolerating even lower oxygen concentrations.

### Alashen 1b Biofacies (lower NP12)

The trend from well-ventilated conditions at the base of the Alashen Formation to lower oxygen concentrations continues into the Alashen 1b Biofacies, with an increase in abundance of species of cluster A, and decreasing abundances of the species of cluster E (Fig. 4). Some species of cluster A reach their peak abundance at the top of the Alashen Formation, also suggesting limiting oxygen concentrations for *Cibicidoides* cf. *decoratus* and *Anomalinoides* cf. *praeacutus*. The high abundance of cluster D species also shows conditions intermediate between well-oxygenated (cluster E) and low oxygen conditions (cluster A), because cluster D contains species that are assumed to be adapted to mesotrophic conditions and can possibly survive lower oxygen concentrations during part of the year. A carbon isotopic offset exists between the endobenthic and epibenthic species, as would be expected for species living at different depths in the sediment (McCorkle et al., 1985).

### Aktulagay 1 Biofacies (middle NP12)

This distinct biofacies occurs in the stratigraphic interval of the Aktulagay section in which the sapropel beds are most prominent and common. Unfortunately, the sapropel beds themselves do not contain calcareous foraminifera at Aktulagay (King et al., 2013) and no samples from the sapropels are included in this study. The high abundance of cluster A species and low abundances of species of clusters B, D and especially E, the high loading on the first DCA axis and lower species richness and Shannon Diversity, all suggest dysoxic conditions at the seafloor. The cluster A species are assumed to occur in high relative abundances because of the absence of most other species not able to resist low oxygen conditions. The absence of ostracods is consistent with this interpretation, as ostracoda are generally less resistant to low-oxygen conditions than the most resistant of benthic foraminifera (Gebhardt and Zorn, 2008). Rising abundance of cluster C species, especially *Bulimina aksuatica*, suggests increased food fluxes. The high abundance of organic matter on the sea floor, together with low-oxygen conditions results in deposition of sapropels (e.g. Calvert and Pedersen, 1993). Rising $\delta^{13}C_{endobenthic}$ values together with a stable $\delta^{13}C_{epibenthic}$ suggest that endobenthic species migrated to the sediment-water interface during deposition of this unit (e.g. McCorkle et al., 1985). At 15.95 m, endobenthic and epibenthic $\delta^{13}C$ have become almost identical. In eutrophic environments, oxygenation controls the vertical position of endobenthic foraminifera in the sediment (Jorissen et al., 1995). Rising abundance of species of cluster C therefore suggests that the vertical migration of endobenthic species is linked to lower oxygen concentrations, even in between the sapropel deposition.

**Aktulagay 2 Biofacies (top NP12 to NP13)**

Lithostratigraphic units B1 and B2 are separated from each other by a hiatus of at least ca. 55 kyr, corresponding to a prominent, deeply burrowed omission surface. This level is interpreted as a combined sequence boundary and transgressive surface, based on the re-appearance of carbonate-rich sediments and an increase in nannofossil and benthic foraminiferal productivity and diversity (King et al., 2013). The high abundance of cluster C taxa and the high loadings on the second DCA axis are assumed to indicate a high (transient) food supply, but not necessarily related to low oxygen concentrations. Especially *E. minuta* and *A. aragonensis* are very common at 20.25 m (highest loading on DCA axis 2) and have been interpreted before as reacting opportunistically in episodic food-rich environments, without low oxygen conditions (D'haenens et al., 2012). The high BFN, together with nearly constant PFN, from 19.45 to 20.25 m, further support the assumed opportunistic behavior of *E. minuta* and *A. aragonensis*, rather than a decrease in abundance of other species. This biofacies is therefore interpreted as characteristic of episodic (possibly seasonal) food supply to the basin.

The offset between the $\delta^{13}$C value of *B. aksuatica* and *U. elongata* suggests deep and shallow endobenthic living positions, respectively. This offset is, however, not present in the sample at 9.00 m. This can indicate that *B. aksuatica* lives at a deeper living position in the Aktulagay 1 (deep endobenthic) than in the Alashen 1 Biofacies (shallow endobenthic, like *U. elongata*). Oxygen limitation was not severe during deposition of the Alashen 1 Biofacies. In well-oxygenated conditions, the trophic level controls the living position of endobenthic taxa (deeper living position if more food reaches the deep habitat; Jorissen et al., 1995). Possibly, the lower food supply in the Alashen 1 Biofacies causes *B. aksuatica* to live at a shallower depth than in the Aktulagay 2 Biofacies. This suggests more eutrophic conditions in the Aktulagay 2 Biofacies.

## 5.3.  Paleoenvironmental reconstruction

The Alashen 1 Biofacies (~54-52.5 Ma) is composed of benthic foraminifera suggesting oligo- to mesotrophic deep outer neritic (~200-250 m) conditions. During deposition of the lower part of the Alashen Formation, oxygen concentrations appear not to be limiting benthic foraminiferal assemblages. However, a gradual increase in benthic foraminifera tolerant of lower oxygen conditions suggests decreasing sea-floor oxygenation.

In this interpretation, the decreasing oxygen concentration in the Alashen 1 Biofacies culminates in low oxygen concentrations and high food availability in the Aktulagay 1 Biofacies (52.5-52 Ma). This part of the section contains four non-calcareous (possibly due to secondary decalcification) sapropel beds suggesting possible transient anoxic bottom water conditions. Periods of oxygen deficiency and deposition of organic-rich layers are frequently associated with transgressive settings (e.g. Hallam and Bradshaw, 1979; Speijer and Wagner, 2002; Schulte et al., 2011). This link has also been proposed for the early Eocene Peri-Tethys sapropels (e.g. Gavrilov and Muzylev, 1991; Gavrilov and Kopaevich, 1996), also present in the Aktulagay Formation. A sequence stratigraphic interpretation for the Aktulagay section supports this for the lowermost sapropel, at the base of unit B1, which is interpreted as a sequence boundary, based on an abrupt lithologic shift from hemipelagic sediments to interbedded clay and marly clay with sapropel beds (King et al., 2013). Other studies suggest that transgressions may flood productive delta and coastal plain settings, transporting the plant debris and nutrients to the sea. High plankton productivity occurs because of the nutrients accumulated in the surface ocean. Increased productivity can cause an expansion of the oxygen minumum zone, enhancing preservation of organic matter (Jenkyns, 1980; Thurow et

al., 1992). Because of the higher export of $^{12}C$ to the ocean floor, $\delta^{13}C$ signatures of planktic foraminifera, if present, rise (Oberhänsli and Beniamovski, 2000). For the early Eocene sapropels, Gavrilov and Muzylev (1991) have shown that numerous dinoflagellates, which appear during deposition of these sapropels, are one of the sources of organic matter, together with land-derived organic matter.

The Aktulagay 2 Biofacies occurs when the warmest temperatures in the Eocene were reached (52-50 Ma, last part of the EECO). In this unit, especially from 19.45 to 20.25 m, the abundant occurrence of assumed high-productivity marker taxa, and the inferred deep habitat of *B. aksuatica* suggest a high organic flux to the sea floor. This interpretation is supported by higher numbers of planktic and especially benthic foraminifera and the occurrence of large dinocysts (>63 μm). This productivity increase could be episodic, as suggested by the benthic foraminiferal fauna. Oxygen concentrations were not limiting, as assumed based on the high abundance of benthic foraminifera suggesting well-ventilated conditions and the inferred deep microhabitat of *B. aksuatica* and the shallow endobenthic microhabitat of *U. elongata*. The high frequencies of nannofossil taxa *Pontosphaera* spp. and *Braarudosphaera bigelowii* were interpreted by King et al. (2013) to indicate more near-shore conditions. High abundance of the *Homotryblium* dinocyst complex at 20.25 m also suggest near-shore, marginal marine areas with adverse conditions (Brinkhuis, 1994), either hypersaline or low-saline (Dybkjær, 2004; Sluijs et al., 2005).

The environmental conditions in the Aktulagay 2 Biofacies bear similarities with environmental conditions generated by large river plumes during the Holocene in the Eastern Mediterranean Sea, during episodes of a strong monsoonal climate, with alternating dry and wet seasons (e.g. Schmiedl et al., 2010). Prior to construction of the Aswan High Dam, summer floods of the Nile River triggered major phytoplankton blooms along the coast of Egypt, Israel and Lebanon (Hecht, 1992; Herut et al., 2000), also caused lower salinity along the coast of Israel (Hecht, 1992). Opportunistic benthic foraminifera can respond to the rapid deposition of fresh phytodetritus generated by phytoplankton blooms (Gooday, 1988; 1993). In the Mediterranean, this causes lower diversity and higher abundance of the opportunistic *Uvigerina peregrina* during times of increased monsoonal rainfall (Kuhnt et al., 2007, Schmiedl et al., 2010).

We infer that at Aktulagay, the effects of a monsoonal climate can be observed. The interpreted high productivity, coupled with relatively high oxygen concentrations could be generated by seasonal nutrient pulses, provided by rivers. During the remainder of the year, productivity was lower and ventilation provided oxygen to the ocean floor. Coastal markers could be present during seasons in which the fluvial influence was high.

Also floral records show evidence of a monsoonal climate, starting in the early Eocene. Floral records of the early Eocene of West-Kazakhstan show a change from a humid paratropical climate with uniform precipitation during the year, to a more monsoon-like climate, humid in the summer period (Akhmetiev and Beniamovskii, 2009; Akhmetiev, 2010). The change to a marine ecosystem occasionally influenced by freshwater input from large river plumes and episodic mixing of the water column possibly expresses the transition to the seasonal monsoon climate. This climate change might be related to the warmest global temperatures during the EECO.

## 5.4. Environmental comparison with the North Sea Basin succession

Schmitz et al. (1996) described benthic foraminifera from the Albæk Hoved section in Denmark and divided the succession in paleo units A to G. The Alashen 1a Biofacies can be correlated to the Paleo-units A to C in the Albæk Hoved section (North Sea Basin

nannoplankton subzones I, II and IIIa1). Deposition appears to start with a much lower sedimentation rate in the Albæk Hoved section, as NSB subzones I and II only contain 0.5 m there, compared with 2 to 3 m of deposits in Aktulagay. The non-calcareous agglutinating foraminifera found in unit A might be relics from the latest Paleocene and earliest Eocene (Schmitz et al., 1996). Lowering of the percentage of non-calcareous benthic foraminifera and rising of the %P suggests a sea-level rise during deposition of paleo unit B. Paleo unit C at Albæk Hoved shows high abundance of calcareous nannoplankton and planktic foraminifera and high diversity of calcareous nannoplankton. This was interpreted as reflecting the greatest water depth and more open water exchange with the world's oceans. At the same time also Aktulagay shows an assemblage suggesting well-oxygenated conditions.

The time-equivalent of the Alashen 1b Biofacies in the Albæk Hoved section is paleo unit D and the first part of unit E (NSB NP subzones IIIa2-IV). Unit D shows low %P (<10 %), decrease in nannofossil abundance and fluctuating and unusually negative foraminiferal $\delta^{18}O$. This was interpreted by the authors to reflect lower surface salinity with low productivity due to a more isolated North Sea Basin. Paleo unit E reflects a return to more open water exchange in the North Sea Basin. At the same time in Aktulagay, the Alashen 1 Biofacies is interpreted to show gradually decreasing oxygen concentrations. While the more restricted nature of the record might explain the lower oxygen concentrations, the return to more open marine conditions is not recorded in Aktulagay. Contrarily, the oxygen concentration is interpreted to even decrease further in the Aktulagay 1 Biofacies. From this point on, the two basins seem to show a different evolution.

The middle and upper part of unit E and the lower part of unit F in the Albæk Hoved section, correlating to the Aktulagay 1 Biofacies, show an increase in nannofossil abundance and %P, suggesting a new rise in sea level and more open water exchange. This is in contrast to what is found in Aktulagay, where the Aktulagay 1 Biofacies is inferred to show lower oxygen concentrations and higher productivity, even outside the sapropels. The sapropel layers that were found in Aktulagay are also represented in the North Sea Basin, representing short anoxic episodes in the otherwise well oxized bottom environment (Heilmann-Clausen et al., 1985; King et al., 2013). Corresponding to one of the sapropels, an abundance peak of *Bulimina aksuatica* has been found (Schmitz et al., 1996), one of the species that is also more abundant close to the sapropels in Aktulagay.

The last differentiated biofacies in Aktulagay, the Aktulagay 2 Biofacies, corresponds in time to the interval from the upper part of paleo unit F to the lower part of the Lillebælt Formation. In the upper part of unit F, nannofossil assemblages are moderately diversified (relative to the rich associations before). The %P decreases slightly later, at the base of unit G, to less than 50 %, possibly reflecting a sea-level fall. The Lillebælt Formation is interpreted as a replacement of open marine by marginal marine sediments, with %P < 10 % and very low nannoplankton abundance. These two periods are separated from each other by increased nannofossil abundance and diversity close to the top of NP12, progressively rising to the top of the Røsnæs Clay. The more marginal marine conditions and low sea-level can correspond to the more coastal position and river influence in Aktulagay at the same time. The shorter period of higher sea-level is possibly missed in Aktulagay due to the low sample resolution.

## 6. Conclusions

An expanded early Eocene quantitative faunal and stable isotopic (C, O) record including the EECO was studied in the Aktulagay section, Kazakhstan. The section features a sequence of sapropel beds, correlated throughout the Peri-Tethys. High abundance of *Pulsiphonina prima* and *Paralabamina lunata* and high diversity in the earliest part of the environmental record

(~54 Ma; NP11) suggest deposition in well-ventilated oligo- to mesotrophic bottom water with a depth of ~200-250 m. From 53.5 Ma onwards, oxygen concentrations are interpreted to start to decrease and the trophic level starts to increase.

Lower diversity and dominance of *Anomalinoides acutus* and *Lenticulina* spp. suggest dysoxic bottom water conditions at ~52.5-52 Ma (middle NP12). This is supported by rising $\delta^{13}C_{endobenthic}$ values, which could indicate that endobenthic species were migrating to the sediment-water interface. High abundance of *Bulimina aksuatica* suggests an increased food flux to the sea floor. The combination of low oxygen concentrations and high food flux are associated with the deposition of sapropels in this unit. The formation of the sapropels and low oxygen conditions might be associated with a transgression with flooding of lowlands, causing increased influx of nutrients and land-derived organic material.

During the peak period of the EECO, from ~52 Ma to 50 Ma (top NP12-NP13), high abundances of benthic foraminifera, especially *Epistominella minuta,* suggest an oligotrophic environment with transient pulses of phytodetritus and moderate ventilation. A stronger continental influence, as inferred from calcareous nannoplankton and dinoflagellate abundances, can be caused by large river plumes reaching the area, caused by a monsoonal climate. Apart from the long-term climate change, also changing paleogeography, with variable connections to the Tethys, Atlantic and Arctic Ocean, could have contributed to the long-term period of dysoxia and anoxia during deposition of the sapropel beds at the Peri-Tethyan seafloor.

The evolution of the basin is largely similar to the evolution of the North Sea Basin, as observed in Denmark. These similarities suggest that these basins were indeed connected during the early Eocene.

## Acknowledgments

## 7.    References

Akhmetiev, M.A., 2010. Paleocene and Eocene floristic and climatic change in Russia and Northern Kazakhstan. Bulletin of Geosciences 85 (1), 77-94.

Akhmetiev, M.A., 2011. Problems of Paleogene stratigraphy and paleogeography in the middle latitudes of Eurasia. Russian Geology and Geophysics 52 (10), 1075-1091.

Akhmetiev, M.A., Beniamovskii, V.N., 2009. Paleogene floral assemblages around epicontinental seas and straits in Northern Central Eurasia: proxies for climatic and paleogeographic evolution. Geologica Acta 7 (1-2), 297-309.

Aubert, J., Berggren, W.A., 1976. Paleocene benthic foraminiferal biostratigraphy and paleoecology of Tunisia. Bulletin des Centre de Recherches exploration-production Elf-Aquitaine Pau 10, 379-469.

Berggren, W.A., Aubert, J., 1975. Paleocene benthonic foraminiferal biostratigraphy, paleobiogeography and paleoecology of Atlantic—Tethyan regions: Midway-type fauna. Palaeogeography, Palaeoclimatology, Palaeoecology 18 (2), 73-192.

Brinkhuis, H., 1994. Late Eocene to Early Oligocene dinoflagellate cysts from the Priabonian type-area (Northeast Italy): biostratigraphy and paleoenvironmental interpretation. Palaeogeography, Palaeoclimatology, Palaeoecology 107 (1–2), 121-163.

Brotzen, F., 1948. The Swedish Paleocene and its foraminiferal fauna. Sveriges Geologiska Undersökning, Ser. C 493, 1-140.

Bugrova, E.M., 2005. Praktičeskoe rukovodstvo po mikrofaune. Tom 8. Foraminifery kajnozoâ. VSEGEI Press, Saint Petersburg, Russia (in Russian, with English abstract).

Calvert, S., Pedersen, T., 1993. Geochemistry of Recent oxic and anoxic marine sediments: Implications for the geological record. Marine Geology 113 (1-2), 67-88.

Charisi, S.D., Schmitz, B., 1996. Early Eocene Palaeoceanography and palaeoclimatology of the eastern North Atlantic: stable isotope results for DSDP Hole 550. In: Knox, R.W.O'B., Corfield, R.M., Dunay, R.E. (Eds.), Correlation of the Early Paleogene in Northwest Europe. Geological Society Special Publications 101. The Geological Society, London, UK, pp. 457-472.

Clemmensen, A., Thomsen, E., 2005. Palaeoenvironmental changes across the Danian-Selandian boundary in the North Sea Basin. Palaeogeography, Palaeoclimatology, Palaeoecology 219 (3-4), 351-394.

Corliss, B.H., Chen, C., 1988. Morphotype patterns of Norwegian Sea deep-sea benthic foraminifera and ecological implications. Geology 16 (8), 716-719.

Corliss, B.H., Honjo, S., 1981. Dissolution of deep-sea benthonic foraminifera. Micropaleontology 27 (4), 356-378.

Cramer, B.S., Aubry, M.-P., Miller, K.G., Olsson, R.K., Wright, J.D., Kent, D.V., 1999. An exceptional chronologic, isotopic, and clay mineralogic record of the latest Paleocene thermal maximum, Bass River, NJ, ODP 174AX. Bulletin de la Société Géologique de France 170 (6), 883-897.

Cramer, B.S., Wright, J.D., Kent, D.V., Aubry, M.-P., 2003. Orbital climate forcing of $\delta^{13}C$ excursions in the late Paleocene-early Eocene (chrons C24n-C25n). Paleoceanography 18 (4), 1097-1121.

D'haenens, S., Bornemann, A., Stassen, P., Speijer, R.P., 2012. Multiple early Eocene benthic foraminiferal assemblage and $\delta^{13}C$ fluctuations at DSDP Site 401 (Bay of Biscay — NE Atlantic). Marine Micropaleontology 88–89, 15-35.

D'haenens, S., Bornemann, A., Claeys, P., Röhl, U., Steurbaut, E., Speijer, R.P., 2014. A transient deep-sea circulation switch during Eocene Thermal Maximum 2. Paleoceanography 29 (5), 370-388.

Dercourt, J., Gaetani, M., Vrielynck, B., Barrier, E., Biju-Duval, B., Brunet, M.F., Cadet, J.P., Crasquin, S., Sandulescu, M., 2000. Peri-Tethys Palaeogeographical Atlas. Gauthier-Villars, Paris, France.

Dybkjær, K., 2004. Morphological and abundance variations in *Homotryblium*-cyst assemblages related to depositional environments; uppermost Oligocene–Lower Miocene, Jylland, Denmark. Palaeogeography, Palaeoclimatology, Palaeoecology 206 (1–2), 41-58.

Ernst, S.R., Guasti, E., Dupuis, C., Speijer, R.P., 2006. Environmental perturbation in the southern Tethys across the Paleocene/Eocene boundary (Dababiya, Egypt): Foraminiferal and clay mineral records. Marine Micropaleontology 60 (1), 89-111.

Fontanier, C., Mackensen, A., Jorissen, F., Anschutz, P., Licari, L., Griveaud, C., 2006. Stable oxygen and carbon isotopes of live benthic foraminifera from the Bay of Biscay: Microhabitat impact and seasonal variability. Marine Micropaleontology 58 (3), 159-183.

Galeotti, S., Krishnan, S., Pagani, M., Lanci, L., Gaudio, A., Zachos, J.C., Monechi, S., Morelli, G., Lourens, L., 2010. Orbital chronology of Early Eocene hyperthermals from the Contessa Road section, central Italy. Earth and Planetary Science Letters 290 (1-2), 192-200.

Gavrilov, Y.O., Kopaevich, L.F., 1996. Some of the geochemical, biochemical, and biotic consequences of eustatic oscillations. Stratigraphy and Geological Correlation 4, 315-325.

Gavrilov, Y.O., Muzylev, N., 1991. The geochemistry of sapropelite interbeds in the Paleogene of Central Caucasus. Lithology and Mineral Resources 26, 548-559.

Gavrilov, Y.O., Shcherbinina, E.A., Oberhänsli, H., 2003. Paleocene-Eocene boundary events in the northeastern Peri-Tethys. In: Wing, S.L., Gingerich, P.D., Schmitz, B., Thomas, E. (Eds.), Causes and Consequences of Globally Warm Climates in the Early Paleogene. Geological Society of America Special Paper 369. Geological Society of America, Boulder, Colorado, pp. 147-168.

Gebhardt, H., Zorn, I., 2008. Cenomanian ostracods of the Tarfaya upwelling region (Morocco) as palaeoenvironmental indicators. Revue de Micropaléontologie 51 (4), 273-286.

Gooday, A.J., 1988. A response by benthic Foraminifera to the deposition of phytodetritus in the deep sea. Nature 332 (6159), 70-73.

Gooday, A.J., 1993. Deep-sea benthic foraminiferal species which exploit phytodetritus: Characteristic features and controls on distribution. Marine Micropaleontology 22 (3), 187-205.

Hallam, A., Bradshaw, M.J., 1979. Bituminous shales and oolitic ironstones as indicators of transgressions and regressions. Journal of the Geological Society 136 (2), 157-164.

Hammer, Ø., 2014. PAST Reference manual. version 3.02.

Hammer, Ø., Harper, D.A.T., 2006. Paleontological Data Analysis. Blackwell Publishing, Oxford, UK.

Hammer, Ø., Harper, D.A.T., Ryan, P.D., 2001. PAST: Paleontological statistics software package for education and data analysis. Palaeontologia Electronica 4 (1), 4.

Hecht, A., 1992. Abrupt changes in the characteristics of Atlantic and Levantine intermediate waters in the Southeastern Levantine Basin. Oceanologica acta 15 (1), 25-42.

Heilmann-Clausen, C., Nielsen, O.B., Gersner, F., 1985. Lithostratigraphy and depositional environments in the Upper Paleocene and Eocene of Denmark. Bulletin of the Geological Society of Denmark 33, 287-323.

Herut, B., Almogi-Labin, A., Jannink, N., Gertman, I., 2000. The seasonal dynamics of nutrient and chlorophyll a concentrations on the SE Mediterranean shelf-slope. Oceanologica Acta 23 (7), 771-782.

Iakovleva, A.I., 2011. Palynological reconstruction of the Eocene marine palaeoenvironments in south of Western Siberia. Acta Palaeobotanica 51, 229-248.

Iakovleva, A.I., King, C., Steurbaut, E., Ward, D.J., Heilmann-Clausen, C., 2004. Early-Mid Eocene dinoflagellates from the Aktulagay section (Kazakhstan): new information on marine connections between the eastern Peri-Tethys and the North Sea Basin. Abstracts XI IPC 2004 International Palynological Congress, Granada, Spain, Polen 14, 199-200.

Jenkins, D.G., Murray, J.W., 1989. Stratigraphical atlas of fossil foraminifera, second edition. British micropalaeontological society series. Ellis Horwood Limited, Chichester, UK.

Jenkyns, H.C., 1980. Cretaceous anoxic events: from continents to oceans. Journal of the Geological Society 137 (2), 171-188.

Jorissen, F.J., de Stigter, H.C., Widmark, J.G.V., 1995. A conceptual model explaining benthic foraminiferal microhabitats. Marine Micropaleontology 26 (1–4), 3-15.

Katz, M.E., Katz, D.R., Wright, J.D., Miller, K.G., Pak, D.K., Shackleton, N.J., Thomas, E., 2003. Early Cenozoic benthic foraminiferal isotopes: Species reliability and interspecies correction factors. Paleoceanography 18 (2), 1024.

Kennett, J.P., Stott, L.D., 1991. Abrupt deep-sea warming, palaeoceanographic changes and benthic extinctions at the end of the Palaeocene. Nature 353 (6341), 225-229.

King, C., Iakovleva, A.I., Steurbaut, E., Heilmann-Clausen, C., Ward, D.J., 2013. The Aktulagay section, west Kazakhstan: a key site for northern mid-latitude Early Eocene stratigraphy. Stratigraphy 10, 171-209.

Knox, R.W.O'B., Bosch, J.H.A., Rasmussen, E.S., Heilmann-Clausen, C., Hiss, M., de Lugt, I.R., Kasiński, J., King, C., Köthe, A., Słodkowska, B., Standke, G., Vandenberghe, N., 2010. Cenozoic. In: Doornenbal, H., Stevenson, A. (Eds.), Petroleum Geological Atlas of the Southern Permian Basin Area. EAGE Publications B.V., Houten, the Netherlands, pp. 211-223.

Kuhnt, T., Schmiedl, G., Ehrmann, W., Hamann, Y., Hemleben, C., 2007. Deep-sea ecosystem variability of the Aegean Sea during the past 22 kyr as revealed by Benthic Foraminifera. Marine Micropaleontology 64 (3–4), 141-162.

Loeblich, A.R., Tappan, H.N., 1988. Foraminiferal genera and their classification. Van Nostrand Reinhold C., New York, New York.

Lourens, L.J., Sluijs, A., Kroon, D., Zachos, J.C., Thomas, E., Röhl, U., Bowles, J., Raffi, I., 2005. Astronomical pacing of late Palaeocene to early Eocene global warming events. Nature 435 (7045), 1083-1087.

Lynch-Stieglitz, J., Curry, W.B., Slowey, N., 1999. A geostrophic transport estimate for the Florida Current from the oxygen isotope composition of benthic foraminifera. Paleoceanography 14 (3), 360-373.

Martini, E., 1971. Standard Tertiary and Quaternary calcareous nannoplankton zonation. In: Farinacci (Ed.), Proceedings of the 2nd International Conference on Planktonic Microfossils. Tecnoscienza, Rome, Italy, pp. 739-785.

McCorkle, D.C., Emerson, S.R., Quay, P.D., 1985. Stable carbon isotopes in marine porewaters. Earth and Planetary Science Letters 74 (1), 13-26.

McCorkle, D.C., Corliss, B.H., Farnham, C.A., 1997. Vertical distributions and stable isotopic compositions of live (stained) benthic foraminifera from the North Carolina and California continental margins. Deep Sea Research Part I: Oceanographic Research Papers 44 (6), 983-1024.

Nguyen, T.M.P., Petrizzo, M.R., Speijer, R.P., 2009. Experimental dissolution of a fossil foraminiferal assemblage (Paleocene–Eocene Thermal Maximum, Dababiya, Egypt): Implications for paleoenvironmental reconstructions. Marine Micropaleontology 73 (3–4), 241-258.

Oberhänsli, H., Beniamovski, V.N., 2000. Dysoxic bottom water events in the Peri-Tethys during the late Ypresian: A result of changes in the evaporation/precipitation balance in adjacent continental regions. GFF 122 (1), 121-123.

Pearson, P.N., van Dongen, B.E., Nicholas, C.J., Pancost, R.D., Schouten, S., Singano, J.M., Wade, B.S., 2007. Stable warm tropical climate through the Eocene Epoch. Geology 35 (3), 211-214.

Pirkenseer, C.M., Steurbaut, E., Abels, H.A., King, C., Speijer, R.P., 2013. An expanded lower Eocene shelf sequence from the eastern Aquitaine Basin, SW France: biostratigraphy, biofacies, and stable carbon and oxygen isotopes. Newsletters on Stratigraphy 46 (3), 339-361.

Roberts, C.D., LeGrande, A.N., Tripati, A.K., 2011. Sensitivity of seawater oxygen isotopes to climatic and tectonic boundary conditions in an early Paleogene simulation with GISS ModelE-R. Paleoceanography 26 (4), PA4203.

Schmiedl, G., Kuhnt, T., Ehrmann, W., Emeis, K.-C., Hamann, Y., Kotthoff, U., Dulski, P., Pross, J., 2010. Climatic forcing of eastern Mediterranean deep-water formation and benthic ecosystems during the past 22 000 years. Quaternary Science Reviews 29 (23–24), 3006-3020.

Schmitz, B., Claus, H.-C., King, C., Steurbaut, E., Andreasson, F.P., Corfield, R.M., Cartlidge, J.E., 1996. Stable isotope and biotic evolution in the North Sea during the early Eocene: the Albæk Hoved section, Denmark. In: Knox, R.W.O'B., Corfield, R.M., Dunay, R.E. (Eds.), Correlation of the Early Paleogene in Northwest Europe. Geological Society Special Publications 101. The Geological Society, London, UK, pp. 275-306.

Schulte, P., Scheibner, C., Speijer, R.P., 2011. Fluvial discharge and sea-level changes controlling black shale deposition during the Paleocene–Eocene Thermal Maximum in the Dababiya Quarry section, Egypt. Chemical Geology 285 (1–4), 167-183.

Sexton, P.F., Wilson, P.A., 2009. Preservation of benthic foraminifera and reliability of deep-sea temperature records: Importance of sedimentation rates, lithology, and the need to examine test wall structure. Paleoceanography 24 (2), PA2208.

Sexton, P.F., Wilson, P.A., Norris, R.D., 2006. Testing the Cenozoic multisite composite δ18O and δ13C curves: New monospecific Eocene records from a single locality, Demerara Rise (Ocean Drilling Program Leg 207). Paleoceanography 21 (2), PA2019.

Sluijs, A., Pross, J., Brinkhuis, H., 2005. From greenhouse to icehouse; organic-walled dinoflagellate cysts as paleoenvironmental indicators in the Paleogene. Earth-Science Reviews 68 (3–4), 281-315.

Speijer, R.P., 1994. Extinction and recovery patterns in benthic foraminiferal paleocommunities across the Cretaceous/Paleogene and Paleocene/Eocene boundaries. Geologica Ultraiectina 124. Ph.D. Thesis, Faculteit Aardwetenschappen, Universiteit Utrecht, Utrecht, the Netherlands.

Speijer, R.P., Schmitz, B., 1998. A benthic foraminiferal record of Paleocene sea level and trophic/redox conditions at Gebel Aweina, Egypt. Palaeogeography, Palaeoclimatology, Palaeoecology 137 (1–2), 79-101.

Speijer, R.P., Wagner, T., 2002. Sea-level changes and black shales associated with the late Paleocene thermal maximum: Organic-geochemical and micropaleontologic evidence from the southern Tethyan margin (Egypt-Israel). In: Koeberl, C., MacLeod, K.G. (Eds.), Catastrophic Events and Mass Extinctions: Impacts and Beyond. Geological Society of America Special Paper 356. Geological Society of America, Boulder, Colorado, pp. 533-549.

Stassen, P., 2012. The impact of the Paleocene-Eocene Thermal Maximum on benthic foraminiferal shelf communities: Paleoenvironmental reconstructions and stratigraphic correlations. Aardkundige Mededelingen 32. Ph.D. Thesis, Department of Earth and Environmental Sciences, KU Leuven, Leuven, Belgium.

Stassen, P., Thomas, E., Speijer, R.P., 2012a. Restructuring outer neritic foraminiferal assemblages in the aftermath of the Paleocene–Eocene thermal maximum. Journal of Micropalaeontology 31 (1), 89-93.

Stassen, P., Thomas, E., Speijer, R.P., 2012b. The progression of environmental changes during the onset of the Paleocene-Eocene thermal maximum (New Jersey Coastal Plain). Austrian Journal of Earth Sciences 105 (1), 169-178.

Stassen, P., Steurbaut, E., Morsi, A., Schulte, P., Speijer, R.P., 2012c. Biotic impact of Eocene thermal maximum 2 in a shelf setting (Dababiya, Egypt). Austrian Journal of Earth Sciences 105 (1), 154-160.

Steurbaut, E., 1998. High resolution holostratigraphy of Middle Paleocene to Early Eocene strata in Belgium and adjacent areas. Palaeontographica Abteilung A 247, 91-156.

Steurbaut, E., 2011. New calcareous nannofossil taxa from the Ypresian (Early Eocene) of the North Sea Basin and the Turan Platform in West Kazakhstan. Bulletin de l'Institut royal des sciences naturelles de Belgique. Sciences de la Terre 81, 247-277.

Stupin, S., 2008. Analysis of foraminiferal paleocoenoses from the upper Ypresian sapropelic layers of the northeastern Peri-Tethys. Stratigraphy and Geological Correlation 16, 198-203.

Thurow, J., Brumsack, H.-J., Rullkötter, J., Littke, R., Meyers, P., 1992. The Cenomanian/Turonian Boundary Event in the Indian Ocean: a Key to Understand the Global Picture. In: Duncan, R.A., Rea, D.K., Kidd, R.B., von Rad, U., Weissel, J.K. (Eds.), Synthesis of Results from Scientific Drilling in the Indian Ocean. Geophysical Monograph 70. American Geophysical Union, Washington, D. C., pp. 253-273.

Tindall, J., Flecker, R., Valdes, P., Schmidt, D.N., Markwick, P., Harris, J., 2010. Modelling the oxygen isotope distribution of ancient seawater using a coupled ocean–atmosphere GCM: Implications for reconstructing early Eocene climate. Earth and Planetary Science Letters 292 (3–4), 265-273.

Vandenberghe, N., Hilgen, F.J., Speijer, R.P., 2012. The Paleogene Period. In: Gradstein, F.M., Ogg, J.G., Schmitz, M.D., Ogg, G.M. (Eds.), The Geologic Time Scale 2012. Elsevier, Boston, Massachusetts, pp. 855-921.

van der Zwaan, G.J., Duijnstee, I., den Dulk, M., Ernst, S., Jannink, N., Kouwenhoven, T., 1999. Benthic foraminifers: proxies or problems?: A review of paleocological concepts. Earth-Science Reviews 46 (1–4), 213-236.

Van Morkhoven, F.P.C., Berggren, W.A., Edwards, A., 1986. Cenozoic cosmopolitan deep-water benthic foraminifera. Bulletin des Centres de Recherches Exploration-Production Elf-Aquitaine, Memoire 11. Elf Aquitaine, Pau, France.

Widmark, J.G., Malmgren, B.A., 1988. Differential dissolution of upper Cretaceous deep-sea benthonic foraminifers from the Angola Basin, South Atlantic Ocean. Marine Micropaleontology 13 (1), 47-78.

Willems, W., 1988. Iconography of the Ypresian foraminifera of the Belgian basin and description of new benthic species. Bulletin van de Belgische Vereniging voor Geologie 97 (3-4), 385-435.

Zachos, J.C., Stott, L.D., Lohmann, K.C., 1994. Evolution of Early Cenozoic marine temperatures. Paleoceanography 9 (2), 353-387.

Zachos, J., Pagani, M., Sloan, L., Thomas, E., Billups, K., 2001. Trends, rhythms, and aberrations in global climate 65 Ma to present. Science 292 (5517), 686-693.

Zachos, J.C., Dickens, G.R., Zeebe, R.E., 2008. An early Cenozoic perspective on greenhouse warming and carbon-cycle dynamics. Nature 451 (7176), 279-283.

Zachos, J.C., McCarren, H., Murphy, B., Röhl, U., Westerhold, T., 2010. Tempo and scale of late Paleocene and early Eocene carbon isotope cycles: Implications for the origin of hyperthermals. Earth and Planetary Science Letters 299 (1–2), 242-249.

## Appendix A.

This appendix summarizes ecological data of earlier studies to provide an interpretation of the ecological significance of each cluster.

## Appendix B.

Tab 1: Sampling positions and sample numbers according to this publication and the AK numbering of King et al. (2013).

Tab 2: Overview of semi-quantitative data (iron-rich concretions, ostracods, dinoflagellates, preservation), general faunal indices (%P, PFN, BFN), sample size and picked fraction.

Tab 3: Overview of stable isotopic data. For each sample, taxonomy, number of specimens, size fraction, whether or not the samples underwent ultrasonic treatment, the $\delta^{13}C$, $\delta^{18}O$ value and standard deviation and the $CO_2$ pressure in the mass spectrometer are indicated.

Tab 4: Benthic foraminiferal relative abundances >2.5 % are given, as well as the number of specimens counted in each sample.

Tab 5 Values of Taxa, Shannon and Buzas and Gibson's Evenness diversity indices for all the analyzed samples.

Tab 6: Sample loadings for the Q-mode DCA on the first two axes.

Tab 7: Alphabetical list of taxa observed in this study. The second column includes likely junior synonyms for the species in the first column.
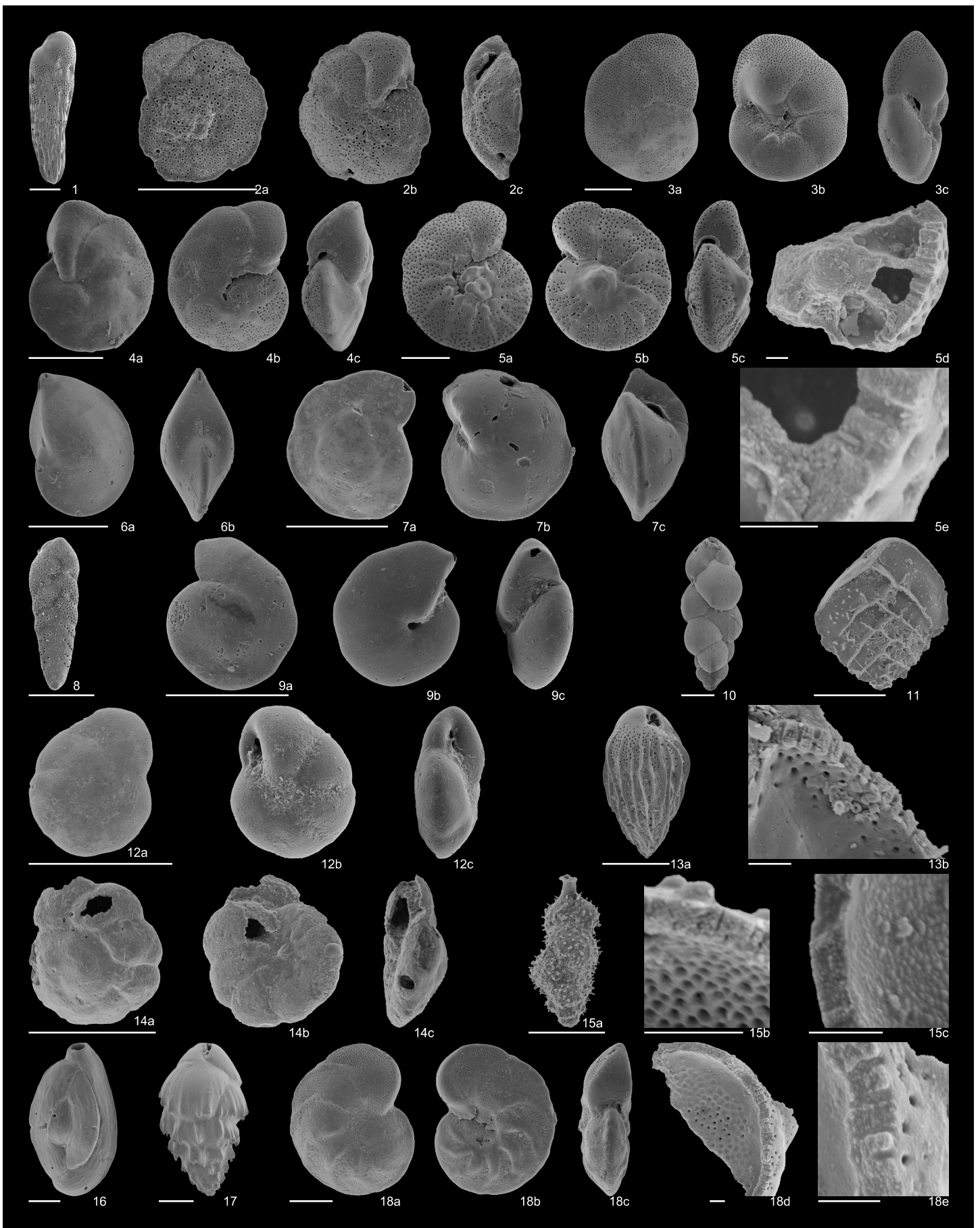
Plate 1. SEM micrographs. The scale bar represents 100 μm except for close-ups and broken samples to illustrate preservation. Sample origin of the specimen given between square brackets. Faunal cluster A: 1) *Loxostomoides applinae* [13.25 m], 2abc) *Cibicidoides* cf. *decoratus* [c.11.9 m], 3abc) *Valvulineria scrobiculata* [13.25 m], 4abc) *Anomalinoides* cf. *praeacutus* [12.75 m], 5abc) *Anomalinoides acutus* [21.5 m], 5de) *Anomalinoides acutus* [23.15 m] (scale bar 10μm) 6ab) *Lenticulina* sp. [c.11.9 m], 7abc) *Oridorsalis plummerae* [c.11.9 m]. Faunal cluster B: 8) *Coryphostoma* sp. [c.11.9 m], 9abc) *Valvalabamina planulata* [c.11.9 m]. Faunal cluster C: 10) *Uvigerinella*? sp. [21.5 m], 11) *Aragonia aragonensis* [21.5 m], 12abc) *Epistominella minuta* [14.05 m], 13a) *Bulimina aksuatica* [14.05 m], 13b) *Bulimina aksuatica* [c.15.95 m] (scale bar 10μm) 14abc) *Anomalinoides*? sp. 2 [c.1.45 m], 15a) *Uvigerina elongata* [c.11.9 m], 15bc) *Uvigerina elongata* [21.5 m] (scale bar 10μm), 16) *Quinqueloculina* spp. [17 m], 17) *Bulimina mitgarziana* [21.5 m], 18abc) *Anomalinoides zitteli* [12.75 m], 18de) *Anomalinoides zitteli* [c.2.45 m] (scale bar 10μm).
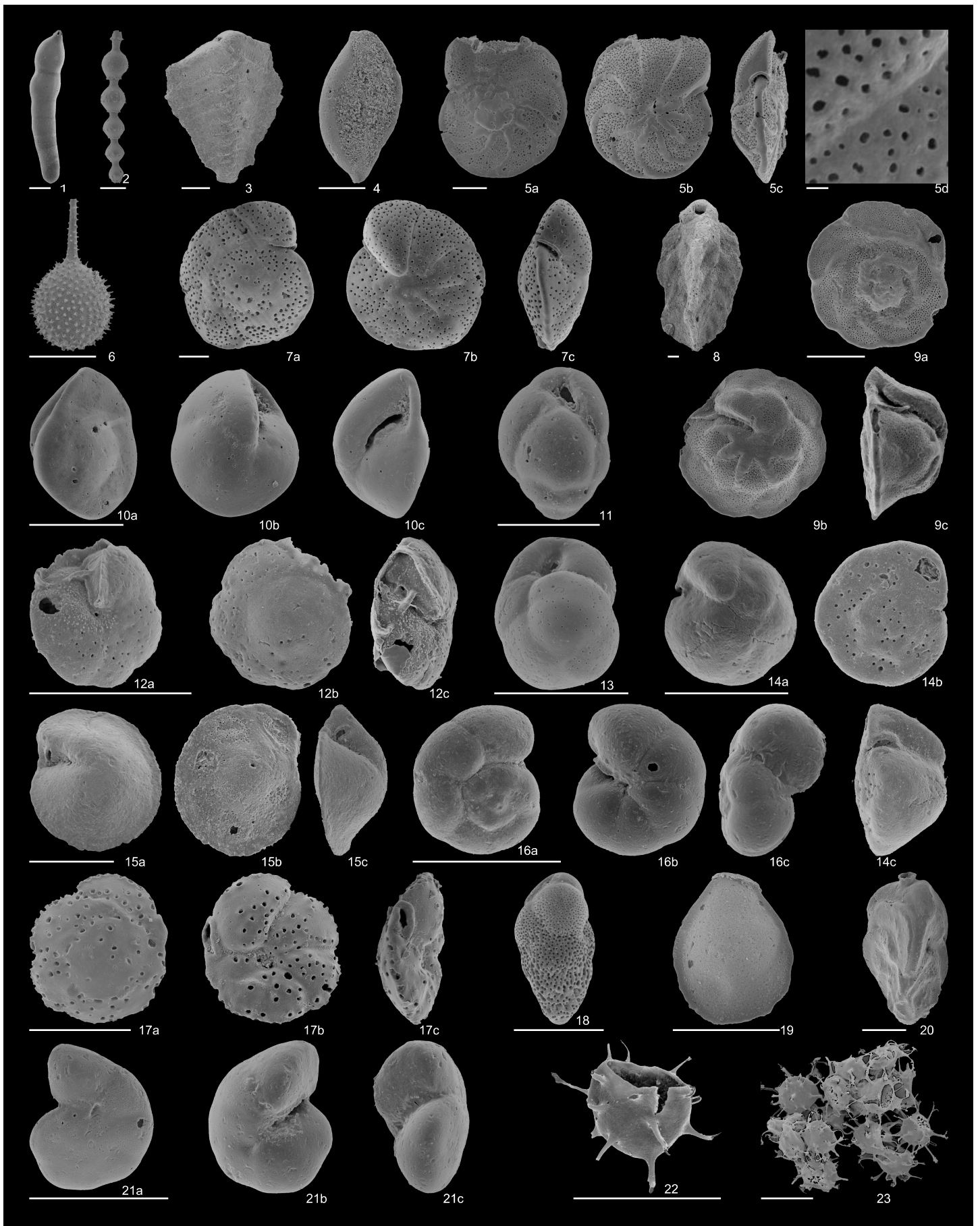
Plate 2. SEM micrographs. The scale bar represents 100 µm except for close-ups. Sample origin of the species given between square brackets. Faunal cluster D: 1) *Dentalina* spp. [c.11.9 m], 2) *Stilostomella* spp. [12.75 m], 3) *Spiroplectinella carinatiformis* [12.75 m], 4) *Spiroloculina* spp. [c.11.9 m], 5abc) *Cibicidoides decoratus* [12.75 m], 5d) *Cibicidoides decoratus* [17 m] (scale bar 10µm), 6) *Lagena* spp. [13.25 m], 7abc) *Cibicidoides rigidus* [12.75 m], 8) *Tritaxia midwayensis* [c.11.9 m], 9abc) *Nuttallides truempyi* [c.11.9 m], 10abc) *Alabamina obtusa* [c.11.9 m], 11) *Turrilina brevispira* [12.75 m]. Faunal cluster E: 12abc) *Paralabamina lunata* [c.11.9 m], 13) *Globocassidulina subglobosa* [c.11.9 m], 14abc) *Cibicidoides bembix* [0.55 m], 15abc) *Osangularia plummerae* [0.55 m], 16abc) *Gyroidinoides octocameratus* [c.11.9 m], 17abc) *Pulsiphonina prima* [c.11.9 m], 18) *Bulimina simplex* [13.25 m], 19) *Seabrookia lagenoides* [3.4 m], 20) *Pseudouvigerina triangularis* [0.55 m], 21abc) *Valvalabamina depressa* [c.11.9 m]. 22) dinoflagellate cyst [19.45 m], 23) group of dinoflagellate cysts [19.45 m].